Journal of GeoEngineering, Vol. 17, No. 2, pp. 89-101, June 2022
http://dx.doi.org/10.6310/jog.202206_17(2).3

DYNAMIC RESPONSE OF SOIL-PILES-MATTRESS-SLAB AND SOIL-PILES-SLAB SYSTEMS UNDER SEISMIC LOADING

Yassamina Neghmouche [1], Salah Messioud [2*], and Daniel Dias [3]

ABSTRACT

This paper presents the dynamic response of soil-piles-mattress-slab and soil-piles-slab systems under seismic loading. In this context, a three-dimensional numerical model using finite elements is proposed; the piles of two systems are embedded in a soft soil. The reinforced soil is surmounted by a load-transfer mattress setup at the rigid piles head level. The piles are embedded in the soft soil and are perfectly connected to a 0.6 m thick slab. The soil-piles-mattress-slab and soil-piles-slab systems are subjected to a horizontal seismic loading. The soil and the mattress are modeled by volume elements, the rigid piles and piles are modeled by beam elements and the slab is by structural elements. The formulation is based on the direct method and the calculations are done considering elastic and elasto-plastic behaviors for the soil mass. The obtained results are compared in terms of horizontal displacements and internal stresses according to the piles length. The obtained results show the effectiveness of the soil-piles-mattress-slab system, the load transfer mattress constituted an energy dissipation zone for the two behaviors. The embedding at the head of the piles induces very high shear forces and bending moments at the level of the pile-structure connection. These efforts could damage the structure. The soil-piles-mattress-slab system eliminates these major efforts at the head of the rigid piles by separating the structure with a mattress. The non-linearity of the ground must be taken into account for further study.

Key words: Soil-structure interaction, piles, mattress, dynamic response.

1. INTRODUCTION

The technique of soil reinforcement by piles, which has been widely used in the construction of industrial structures, slab foundations, and embankments, has experienced tremendous growth in recent years. Several researches considered deep piles-slab foundations or piles-mattress as effective solutions to ensure the stability and security of structures on soft soils and in seismic regions. Improvement soil by rigid piles is traditional technique, consisting of placing a group of vertical piles across a soft soil for the loads transfer to a more rigid layer. The technique has some benefits like its versatility, cost effectiveness and fast construction (Deb and Mohapatra 2013), as well as its technical efficiency both in terms of bearing capacity and reduction of absolute and differential settlements (Jenck *et al.* 2006, 2007, 2009a, 2009b; Hassen *et al.* 2009; Nunez *et al.* 2013; Girout *et al.* 2014; Briançon *et al.* 2015). For the soil reinforcement by piles, a layer of granular soil with good mechanical characteristics (load-transfer mattress) is setup. It allows the reduction and homogenization of the slab settlements. A geo-synthetic can be installed at the mattress base contributing to the load transfer by membrane effect.

The use of soil-piles-mattress-slab in seismic zones is an interesting concept with respect to a seismic load; this reinforcement system is similar to an insulation system at the base of the structure (Mayoral *et al.* 2006; Hatem. 2009; Okyay *et al.* 2010). Deep piles-slab foundations and piles-mattress reinforcements are part of vertical elements. In order to understand the dynamic response of a structure under seismic loading, it is therefore important to study the dynamic behavior of piles-mattress. An essential step in the seismic design of structures is to study the influence of the soil-structure interaction on the seismic foundations response (Tajimi 1969; Novak and Aboul-Ella 1978; Kagawa and Kraft 1980; Kaynia and Kausel 1982; Gazetas and Dobry 1984; Hatem *et al.* 2009).

Earthquakes are very complex phenomena that should be well considered in estimating the structures safety. The constructions of civil engineering structures, such as nuclear power plants, gas tanks and offshore constructions, in seismic zones and soft soils, require seismic calculations of soil improved by piles (Mohanad al Fash 2009; Messioud *et al.* 2016, 2017). The use of foundations or pile-slab foundations allows to improve the seismic reaction of structures as well as to minimize the seismic risk and increase the soil-structure system damping (McKay 2009; Messioud *et al.* 2019). In addition, the use of foundations resting on soil improved by piles with a transfer mattress interposed at the piles is considered as a better solution in seismic zones. The load-transfer mattress constitutes a dissipation energy zone at the mattress structure interface (Hatem 2009).

Most earthquake engineering researchers consider the soil-structure interaction (SSI) analysis to design structures with foundations (Choi *et al.* 2001; Gueguen *et al.* 2002) or design structures rested on deep foundations. When the seismic response of structures began to be studied, some importance was given to the influence of the soil-structure interaction on the seismic response of foundations and structures. The response of structures to the earthquakes was analyzed by direct approaches (without taking into account the soil-structure interaction effect), the structures

Manuscript received December 8, 2021; revised March 23, 2022; accepted April 28, 2022.
[1] Ph.D. candidate, LGCE Departement of Civil Engineering, University of Jijel, BP98 18000, Algeria.
[2*] Associate Professor (corresponding author), LGCE Departement of Civil Engineering, University of Jijel, BP98 18000, Algeria (e-mail: smessioud@yahoo.fr).
[3] Professor, 3SR Laboratory/Polytech, Grenoble Alpes University, France.

being assumed to be embedded in the soil. This opens a great debate on what variables control the SSI and further increases the need for including the soil-structure interaction in the analyses (Jennings and Bielak 1973). However, as more and more proofs of the importance of soil-structure interaction were brought to light, many researchers and engineers gave a great importance to the influence of soil-structure interaction on the seismic response of foundations. In this context, several numerical modeling with and without absorbing boundaries were used to study the vibration of piles-slab and piles-mattress groups (Sen *et al.* 1985; Xlin Lu *et al.* 2003; Moeso *et al.* 2005; Padrón *et al.* 2007). The dynamic behavior of soil-piles-mattress-structure under dynamic loading was studied by different numerical method, such as, Hatem (2009), Okyay (2010), Messioud *et al.* (2016), Zhuang and Wang (2016, 2018), and Pham and Dias (2019); and their validity was confirmed by small scale model results.

The global method consists of a single-step solution of the dynamic soil-structure interaction, considering the time or frequency domain. The technique is usually based on the finite element method which has a great flexibility and also allows considering non-linear phenomena, such as the elasto-plastic behavior of materials. To obtain the dynamic response, considering a finite element numerical model of a structure rested in the semi-infinite space, artificial boundaries are necessary in order to limit the model's degrees of freedom number. This kind of boundary poses the problem of the energy transmitted by the reflected waves. The waves are reflected at the border of the model instead of being radiated through the underlying soil layers (Hatem 2009; Okay 2010; Messioud *et al.* 2016, 2017). In a real and physical environment, absorbing boundaries allow to absorb the energy of the reflected waves.

This work is oriented towards the qualification and quantification of solicitations and displacements in the soil-piles-slab and soil-piles-mattress-slab systems subjected to seismic loading, in order to study the effectiveness of soil reinforcement systems (soil-piles-mattress-slab) compared to the soil-piles-slab system. For this reason, three-dimensional finite element numerical models with absorbing boundaries are proposed to study the dynamic response of soil-piles-mattress-slab and soil-piles-slab systems under a seismic loading (Figs. 1(a) and 1(b)). For the two systems, the piles are embedded in a coherent soft soil limited by a rigid bedrock. The reinforced soil is surmounted by a load-transfer mattress at the piles head. For the piles-slab system, the piles are perfectly connected to the slab. The soil-piles-mattress-slab and soil-piles-slab systems are subjected to a horizontal seismic loading. The formulation is based on the direct method. The calculations are carried out considering elastic and elasto-plastic behaviors for the soil mass.

2. NUMERICAL MODELS

The geometric characteristics of the model were determined by a parametric study to ensure the correct functioning of the absorbing boundaries. The considered soil volume is contained in a zone of $40 \times 40 \times 15$ m^3. The number of piles for the two systems is equal to 30. The length of the concrete piles embedded in the soft soil is equal to 10 m, and their diameter is 0.3 m. The load-transfer mattress is modeled by volume elements of 0.6 m thickness. The seismic force is applied at the base of the studied systems (base of the hard soil layer). The mechanical properties of the soil layers and transfer mattress are presented in Table 1. The choice of these properties was made considering the works of Okyay (2010) and Messioud *et al.* (2016).

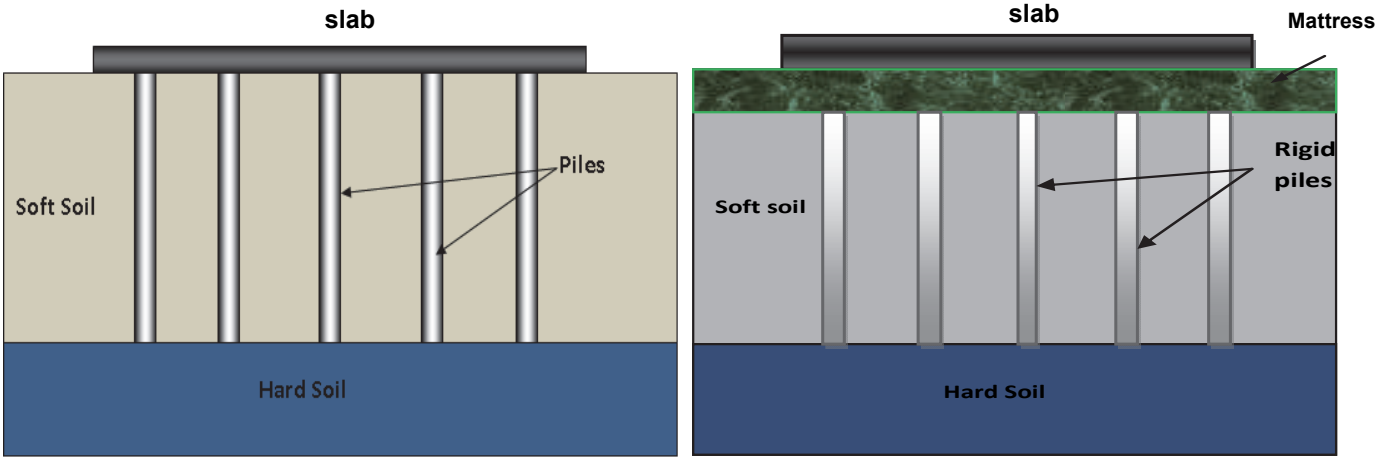

(a) Soil-piles-slab system (b) Soil-piles-mattress-slab system

Fig. 1 Studied systems

Table 1 The mechanical properties of the elements

Parameter	Piles / slab	Mattress	Soft soil	Hard soil
Elastic modulus E (kPa)	25,000,000	50,000	10,000	100,000
Poisson ratio	0.25	0.4	0.4	0.4
Density (kg/m^3)	2,500	2,000	1,800	2,200
Damping coefficient	–	0.5	0.5	0.5
Angle of friction, ϕ (°)	–	25	25	25
Angle of dilatancy, ψ (°)	–	10	10	10
Cohesion, c (Pa)	–	50,000	5,000	5,000

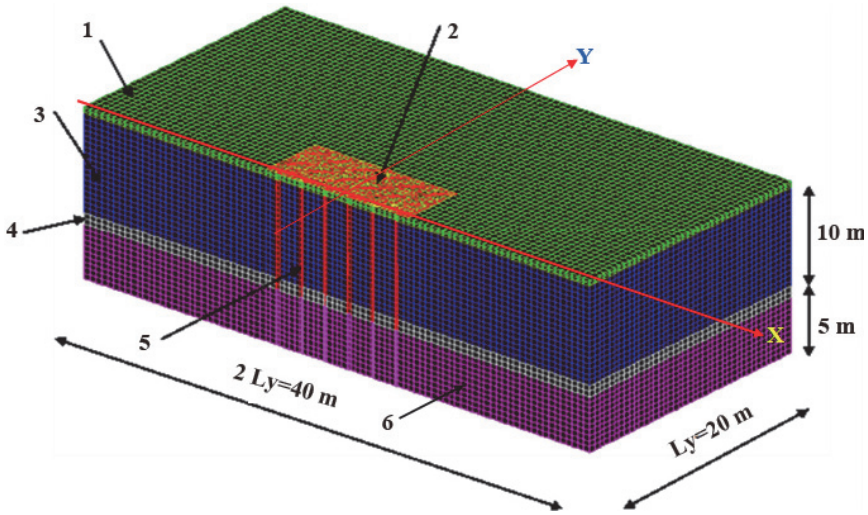

(a) Half numerical model: 1 is mattress; 2 is slab ; 3 and 4 are soft soil layers; 5 is rigid piles; 6 is hard soil layer

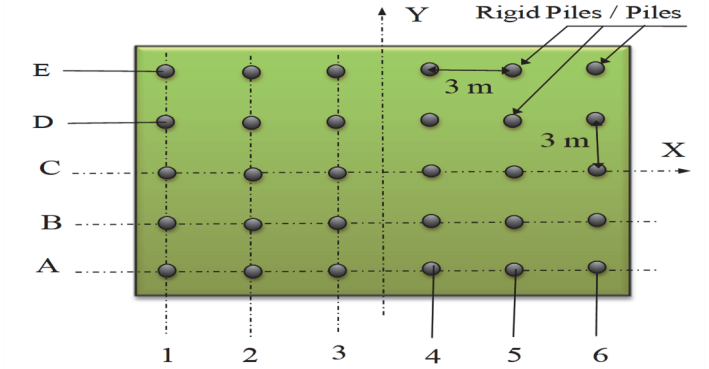

(b) Position of the piles

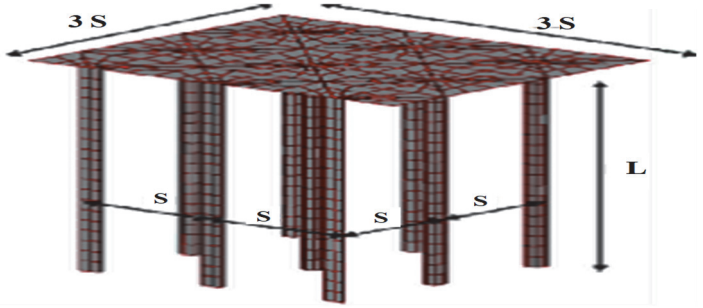

(c) Group of piles (piles-slab)

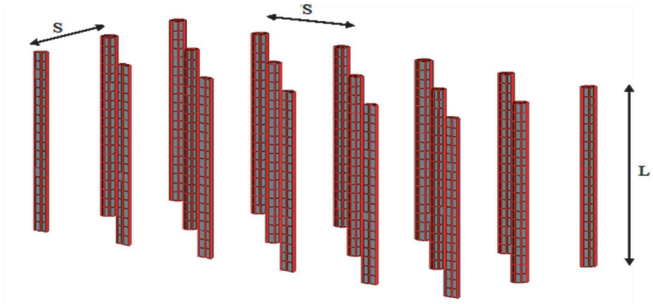

(d) Group of piles (piles-mattress)

Fig. 2 Numerical models

2.1 Numerical Studied Systems

The soft soil layer has a height of 10 m and is rested on a hard soil layer (5 m height). Depending on the geometrical configuration and model type, the piles crossed the compressible soil layer and stopped at 10 m depth. The choice of the size model and element size is consistent with the longer wavelength to minimize the wave distortion effect.

In order to simplify the problem, the soil layers are assumed to be horizontal in a semi-infinite medium. The soil of the site often extends over to high depths, and it is then necessary to introduce an artificial boundary. In the used models, this boundary was set at a depth of 15 m. This boundary allows taking into account the reflected energy distribution transmitted to the substratum (Lysmer and Kuhleneyer 1969). The size mesh elements must be less than one-tenth of the wavelength. Details can be found in Messioud *et al.* (2016, 2017, 2019). The maximum frequency which can be applied depends on the maximum size of the element. Kuhlemeyer and Lysmer (1973) show that the size mesh element must be less than one tenth of the wavelength λ,

$$f = \frac{C_s}{10 \cdot \Delta l} = \frac{\omega}{2\pi}$$

with C_s the shear-wave velocity, Δl the size of the mesh element and ω the circular frequency of excitation.

Free-field boundaries are attributed to the vertical faces and to the bottom face of the numerical model. Paraxial elements are assigned to the free boundaries to answer soil-structure interaction problems and to satisfy the sommerfield conditions. The

seismic loading is applied in the horizontal direction **x** as a signal imposed at the soil base which is considered as perfectly rigid.

2.2 Input Seismic Data

The used seismic signal in this work is the Nice signal (Sun *et al*. 2020). Its accelerogram is presented in Fig. 3(a). It is representative of the French design spectrum (Grange 2008). It has a maximum acceleration equal to 0.33 g. The corresponding Fourier amplitude spectrum is given in Fig. 3(b).

The fundamental frequency of a soil layer can be calculated by the following formula $\omega = 4\ H/V_s$, where V_s is the shear wave velocity in m/s, H is the total depth of the layer soil**.** For small damping values, the resonant frequency is approximately equal to its natural frequency.

For the compressible soil layer, the fundamental frequency is equal to 1.25 Hz.

2.3 Numerical Software Used

Code aster is a free software for numerical simulation in structural mechanics, developed mainly by the "mechanical and acoustic analysis", it is mainly a solver, based on the theory of continuum mechanics, and wish uses the finite element method to solve different types of mechanical, thermal, acoustic, seismic, *etc*.

In order to extract the results using the code aster, we insert two files (geometry file and command file). The geometry file we extract using GMSH software, in which we draw the systems and give the dimensions for each of the elements (soils, piles, mattress and slab), and divide each element into finite elements in the form cubic of the size $1 \times 1 \times 1$ m^3, as shown in the Fig. 2(c). The command file is a set of data related to the mechanical properties of materials and a set of commands for extracting results using the Stanley application. Application STANLEY is a tool for interactive post processing for calculations of Code Aster. This graphic interface gives access to the list of the sizes, to generate the exits for the tools for visualization SALOMÉ (isovaleurs and curves), Gmsh (isovaleurs) and Xmgrace (curves) and launching of those.

3. ELASTIC DOMAIN

3.1 Results and Discussion

The piles, mattress and soil layers were considered as elastic in these simulations. These results for rested piles of the rows A1, A2, and A3 (Fig. 2) are presented in the following section.

Figure 4 shows the variation of the displacement and internal forces at the head of the pile A1 as a function of time. For time duration equals to 14 s with a step of 0.008 s, this figure shows that the internal forces and displacements evolutions are following the seismic loading. The displacements at the head piles of the two systems are identical. The maximum displacement time history is obtained between 7 and 8 second (Fig. 4). The shear force at the pile head of the piles-slab system is greater than the shear force of the piles-mattress system. For the piles-slab system, the bending moment at the pile head is important since this node is perfectly recessed in the slab. However, for the piles-mattress system the bending is almost equal to zero as the node is supposed to be articulated in the mattress and is not connected to the slab. This characteristic shows the effectiveness of the reinforcement system; the moments and the shear forces are eliminated by adding between the slab and the piles head, a granular mattress.

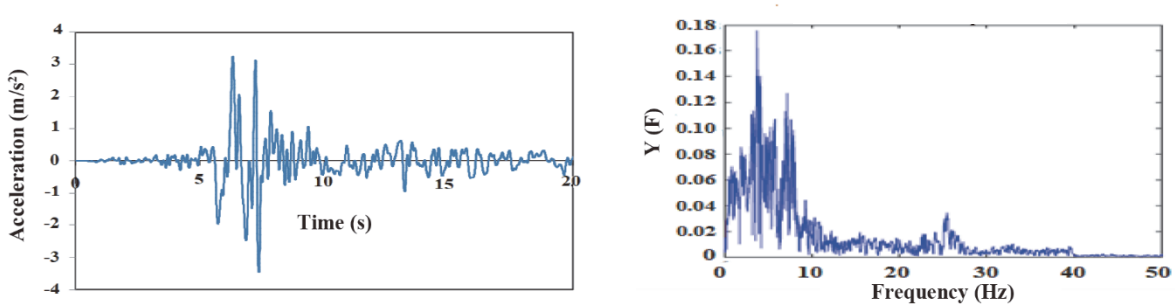

(a) Accelerogram $a(t)$ (b) Fourier amplitude

Fig. 3 Adopted seismic loading of Nice

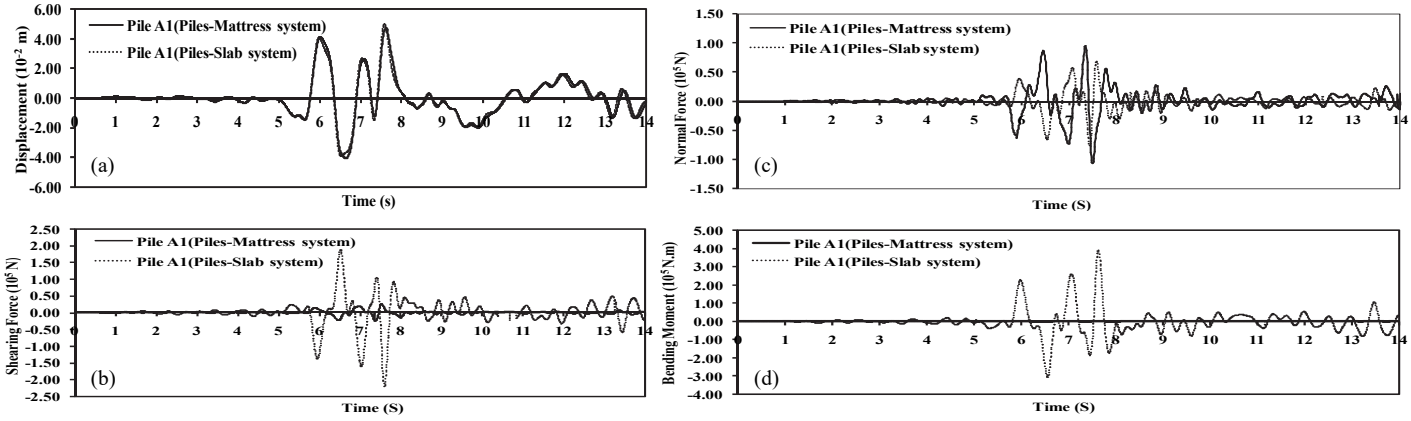

Fig. 4 Displacements and internal forces at the pile heads A1 of the tow systems as a function of time

3.1.1 Displacement

Figure 5 shows the displacements variation of piles A1, A2, and A3 of the two systems as a function of length. The figure shows that the obtained displacements are identical; the displacements at the head and at the bottom of the piles of the piles-mattress system are almost the same. However, the displacement of the pile A3 is greater than the displacement of the pile A2, and the displacement of the latter is greater than the displacement of the pile A1. The same remark for the piles-slab system is observed. The obtained results show that the displacements variation according to the length is linear. The maximum value of displacements is located at the head of the two systems (Piles-slab and Piles-mattress systems, Figs. 5(a) and 5(b)). These results can be caused by the increase of the soil reactions depending on the depth of the piles.

3.1.2 Bending Moments, Normal Forces and Shear Forces

Figure 6 shows that the shear forces in the piles-mattress system are concentrated at the two extremities of the piles. The maximum shear force values shear are obtained at the pile A3 head where the bending moments is zero. Additionally, at a depth of value between 5 and 6 m, the shear forces are equal to zero because this depth corresponds to half of the wave length (Fig. 6(a)). At this depth, the piles bending moment is maximum, the highest value is found for rigid pile A3, because the rigid pile A3 is closest to the center of application of the seismic force. In the piles-slab system (Fig. 6(b)), the maximum values of the shear forces and of the bending moments are located at the A3 head pile. The bending moments are zero as the piles bottom is articulated, and the shear forces are low. The normal force of the pile A3 in the two systems is greater than the A2 ones. The normal force of the latter is greater than A1. The numerical results of the displacements and internal forces of the piles-slab and piles-mattress systems are shown in Table 2.

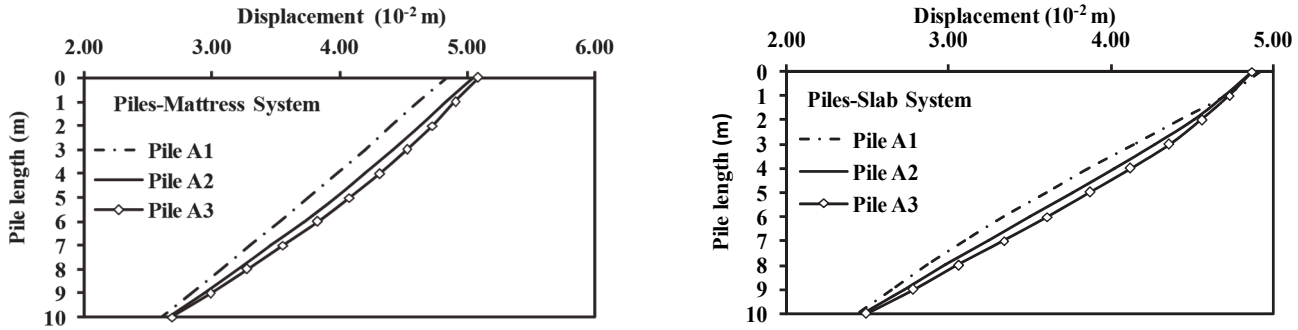

(a) Piles-mattress system (b) Piles-slab system

Fig. 5 Horizontal displacements of the piles A1, A2, and A3

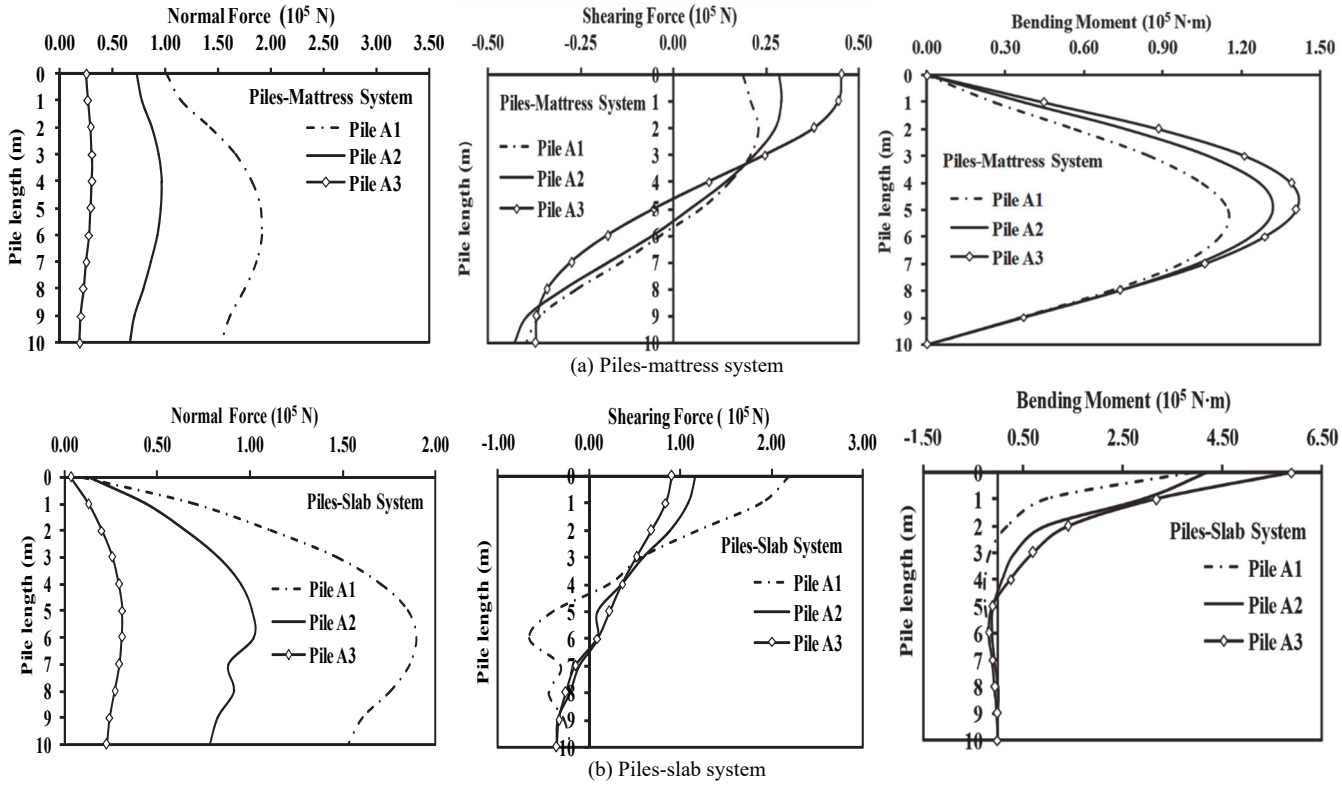

(a) Piles-mattress system

(b) Piles-slab system

Fig. 6 Internal forces of the piles-slab and piles-mattress systems (piles A1, A2, and A3)

Table 2 Numerical results of the piles slab and piles mattress slab systems

			Displacements $\times 10^{-2}$ (m)			Normal forces $\times 10^5$ (N)			Shear forces $\times 10^5$ (N)			Bending moment $\times 10^5$ (N·m)		
			A1	A2	A3	A1	A2	A3	A1	A2	A3	A1	A2	A3
Piles-slab system	Piles length	0 m	4.92	4.87	4.87	– 0.0979	– 0.1350	– 0.0340	2.200	1.1700	0.9030	3.90.30	4.2000	5.9008
		5 m	3.60	3.76	3.87	– 1.8506	– 1.0100	– 0.3128	– 0.0396	0.0875	0.2213	– 0.24.53	– 0.0940	– 0.1100
		6 m	3.34	3.5	3.61	– 1.9045	– 1.0202	– 0.3112	– 0.0657	0.0891	0.0875	– 0.1771	– 0.1085	– 0.1776
		9 m	2.65	2.72	2.78	– 1.6117	– 0.8286	– 0.2443	– 0.2730	– 0.3460	– 0.3339	– 0.0109	0.0058	– 0.0109
		10 m	2.43	2.47	2.49	– 1.5326	– 0.7823	– 0.2295	– 0.2000	– 0.3586	– 0.3594	0.00034	0.00	0.00
Piles-mattress-slab system	Piles length	0 m	4.84	5.05	5.09	– 1.0105	– 0.7289	– 0.2500	0.1872	2.6874	0.4530	0.00082	0.0945	0.00105
		5 m	3.76	3.97	4.08	– 1.9031	– 0.9590	– 0.2937	0.0779	0.0482	– 0.0504	1.1500	1.3203	1.4112
		6 m	3.53	3.72	3.83	– 1.9104	– 0.9227	– 0.2746	– 0.0326	– 0.0518	– 0.1761	1.1200	1.2425	1.2955
		9 m	2.84	2.93	2.99	– 1.6100	– 0.7072	– 0.1991	– 0.3593	– 0.3933	– 0.3683	0.3645	0.03749	0.3680
		10 m	2.61	2.66	2.69	– 1.5311	– 0.6665	– 0.1863	– 0.3950	– 0.4297	– 0.3708	0.00076	0.00072	0.00067

3.1.3 Cross Analysis

In this analysis, the stresses in the three rows of piles A, B and C of two systems are considered. The stresses are calculated at a depth equal to 5m in the three rows of rigid piles. Figure 7 shows the variation of the internal forces in the direction of the seismic signal.

While studying the dynamic response of the piles-mattress-slab and the piles-slab, an increase of the displacements towards the network center for three rows A, B and C can be observed. The behavior in terms of bending moment is the same as the displacements one (Fig. 7(a)), these results show that the piles behave respectively like embedded beams and simply laid.

The evolution of the shear forces from the periphery to the network center is also studied. Although there is a strong reduction of the forces in the piles of the piles-mattress system on the C axis (Fig. 7(a)), the shear forces increase to the center for the piles on the B axis. The shear force on axis A is different, some increase and some decrease. However, for the piles-system Fig. 7(b), the shear forces are reduced on the two rows B and C, where as the shear force increases to the center on the row A. The results show that the increase in shearing force is inversely proportional to the increase in bending moment. Table 3 presents the numerical results for the change of displacement and internal forces in three rows A, B, and C of the piles-mattress and piles-slab systems.

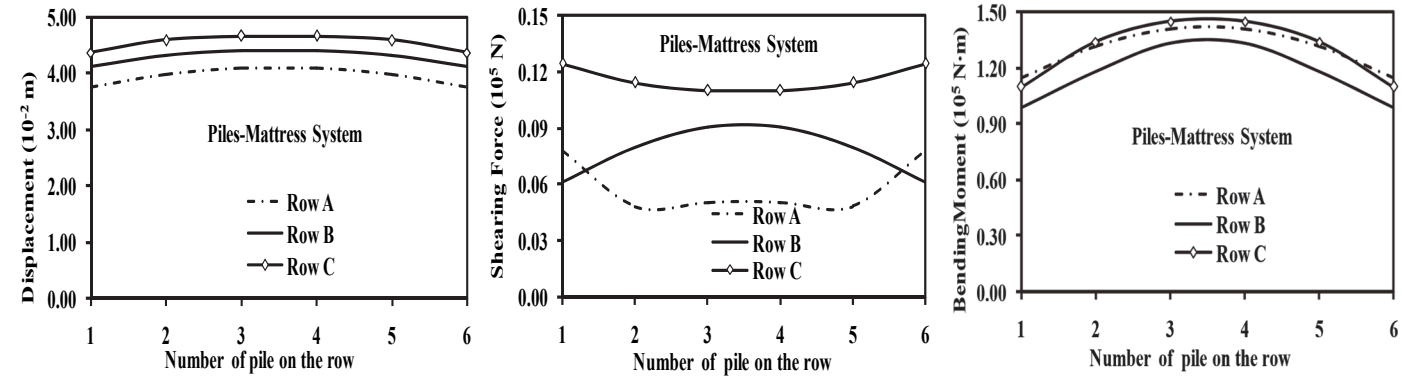

(a) Piles-mattress system

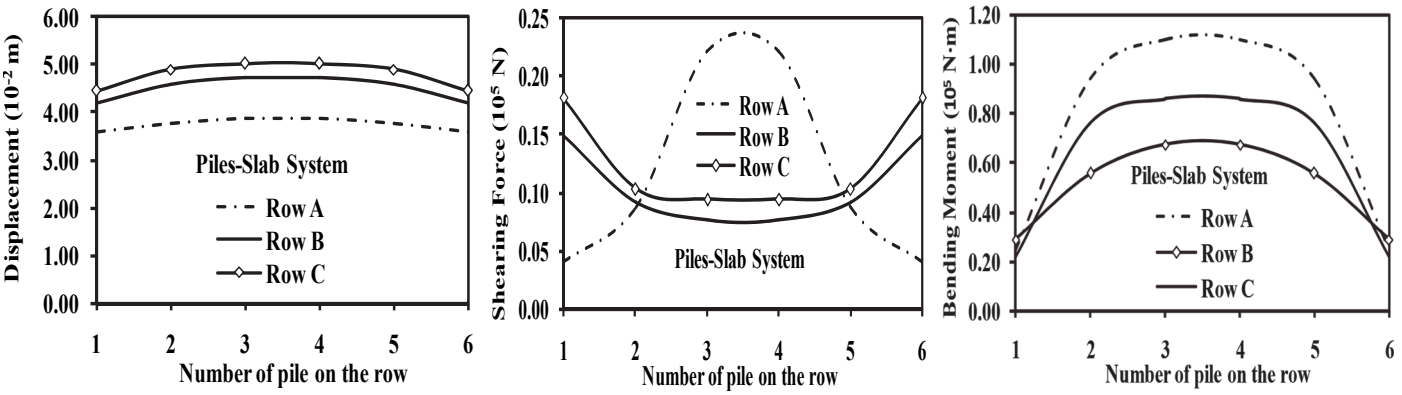

(b) Piles-slab system

Fig. 7 The variation of the displacement and of the internal forces in the rows A, B, and C

Table 3 Results in the rows A, B, and C of the piles-slab and piles-mattress-slab systems

		Piles	Displacements $\times 10^{-2}$ (m)	Bending moments $\times 10^5$ (N·m)	Shear forces $\times 10^5$ (N)
Piles-mattress-slab system	Row A	A1; A6	3.76	1.1500	0.0779
		A2; A5	3.97	1.3203	0.0482
		A3; A4	4.08	1.4112	0.0504
	Row B	B1; B6	4.11	0.9905	0.0613
		B2; B5	4.31	1.1885	0.0798
		B3; B4	4.39	1.3317	0.0903
	Row C	C1; C6	4.36	1.1025	0.1240
		C2; C5	4.58	1.3443	0.1145
		C3; C4	4.65	1.4519	0.1103
Piles-slab system	Row A	A1; A6	3.60	0.2453	0.0396
		A2; A5	3.76	0.0940	0.0875
		A3; A4	3.87	0.1100	0.2213
	Row B	B1; B6	4.18	0.2892	0.1498
		B2; B5	4.58	0.5568	0.0922
		B3; B4	4.72	0.6737	0.0759
	Row C	C1; C6	4.45	0.2165	0.1816
		C2; C5	4.90	0.7612	0.1033
		C3; C4	5.02	0.8587	0.0939

3.1.4 Comparison Between the Piles-Mattress-Slab and Piles-Slab Systems

Figure 8 presents a comparison of the displacements and internal forces for pile A1. In this comparison, the soft soil and mattress are assumed to be compressible with a Young's modulus of 10 and 50 MPa, respectively. The radius of piles is equal to 0.3 m. At the pile head of the piles-mattress system, the normal force is greater than the normal force at the pile head of the piles-slab system (Table 4). The shear force is concentrated at the two ends of the pile. In the piles-slab, the maximum shear force and the maximum moment are located at the head (Table 4).

3.1.5 Influence of the Soft Soil Elastic Modulus

In this section, by varying the elastic modulus of the soft soil from 10 MPa to 50 MPa, Fig. 9 shows its influence on the horizontal displacements of the A1 piles as a pile length function. The maximal displacements are found at the head level with $Dx(Es = 10\ \text{MPa})/Dx(Es = 50\ \text{MPa}) = 0.0484/0.0227 = 2.13$ in the piles-mattress system, and $Dx(Es = 10\ \text{MPa})/Dx(Es = 50\ \text{MPa}) = 0.0497/0.019 = 2.61$ at the pile head of the piles-slab system, and at the bottom of the piles-mattress system $Dx(Es = 10\ \text{MPa})/Dx(Es = 50\ \text{MPa}) = 0.0261/0.0157 = 1.66$ and at the bottom of the piles-slab $Dx(Es = 10\ \text{MPa})/Dx(Es = 50\ \text{MPa}) = 0.0243/0.0130 = 1.87$.

For the piles-mattress system as shown in Fig. 9(b), these displacement ratios show the effectiveness of the reinforcement system. For 10 MPa soils, the displacements are doubled compared to those of 50 MPa, especially at the piles head. For the piles-slab system, the displacements at the piles head are greatly amplified compared to the rigid piles system ones.

Table 4 Results of the piles-slab and piles-mattress-slab systems

		Displacement $\times 10^{-2}$ (m)	Normal forces $\times 10^5$ (N)	Shear forces $\times 10^5$ (N)	Bending moments $\times 10^5$(N·m)
Pile-slab pile A1	0 m	4.92	0.0979	2.2000	3.9030
	5 m	3.6	1.8506	– 0.0396	– 0.2453
	6 m	3.34	1.9045	– 0.0657	– 0.1771
	9 m	2.65	1.6117	– 0.2730	– 0.0109
	10 m	2.43	1.5326	– 0.2000	0.00034
Pile-mattress pile A1	0 m	4.84	1.0105	0.1872	0.00082
	5 m	3.76	1.9031	0.0779	1.1500
	6 m	3.53	1.9104	– 0.0326	1.1200
	9 m	2.84	1.6100	– 0.3593	0.3645
	10 m	2.61	1.5311	– 0.3950	0.00076

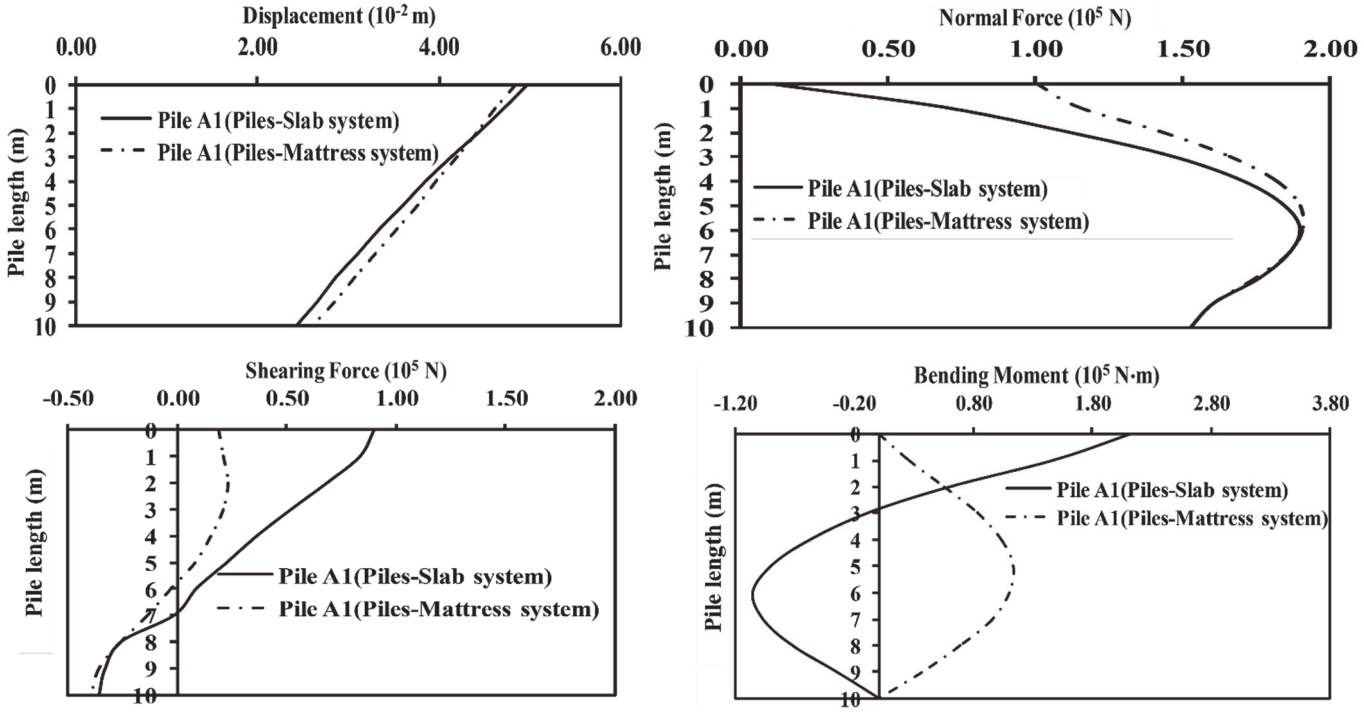

Fig. 8 The comparison between the solicitation of the piles-slab and piles-mattress-slab systems

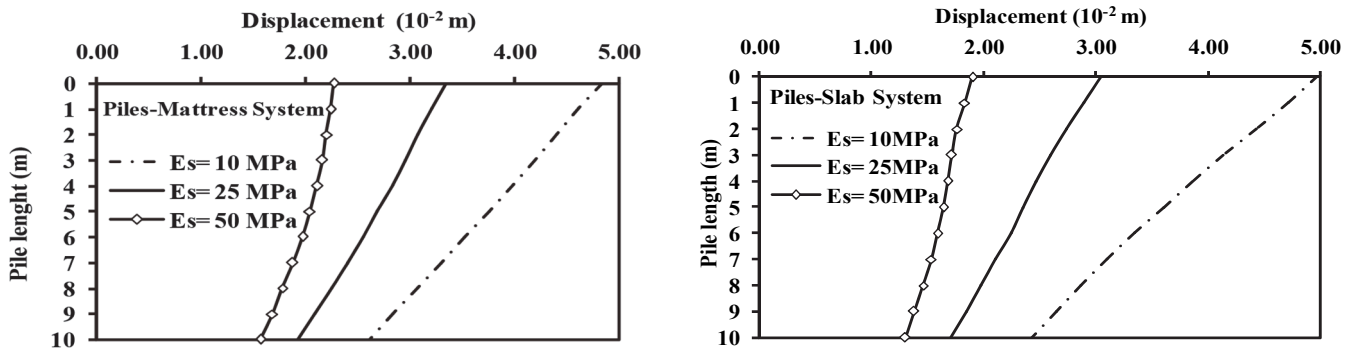

(a) Piles-mattress system (b) Piles-slab system

Fig. 9 Influence of the soft soil modulus on the displacements of the piles-slab and piles-mattress-slab systems

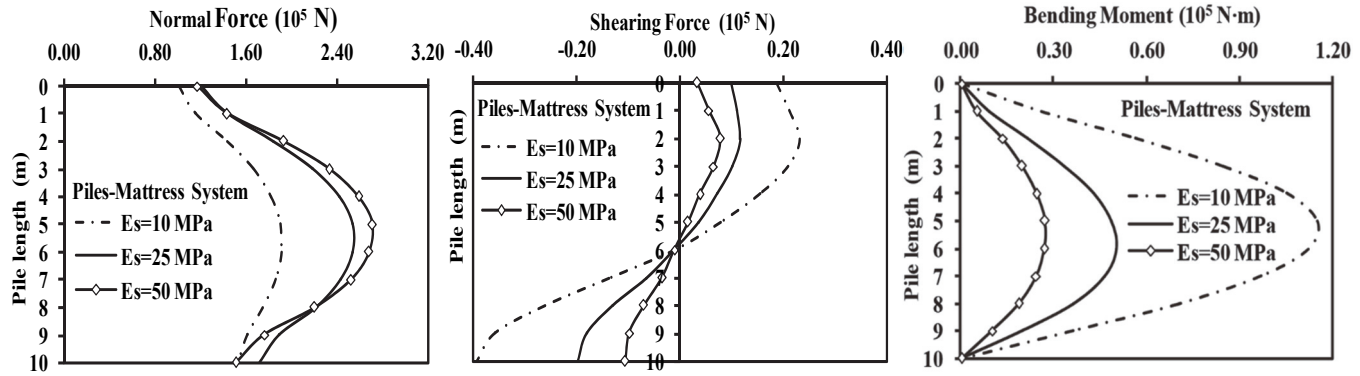

(a) Piles-mattress system

Fig. 10 Influence of the soft soil modulus on the piles-mattress-slab system solicitations

The obtained results show that the soft soil elastic modulus affects considerably the internal forces. A substantial increase of the normal effort and a slight decrease of the bending moment and shear force are observed in Fig. 10. The increase of the soft soil elastic modulus induces an increase of the soil resistance which causes a decrease of the internal forces of the piles-mattress.

3.1.6 Influence of the Mattress Elastic Modulus

An extensive study based on the reference case is done. To simplify the results presentation, the A1 pile of the piles-mattress system is considered by varying the load transfer mattress modulus from 50 to 500 MPa. The obtained results are presented in the following figures.

Figure 11 shows the load transfer mattress stiffness influence on the horizontal rigid pile A1 displacements as a function of the pile length. This figure shows that the maximum displacement is at the head of the pile. This displacement decreases with the mattress stiffness increase. At the $Dx(Em = 50\ \text{MPa})/Dx(Em = 500\ \text{MPa}) = 0.0484/0.0382 = 1.267$ head, the displacement decreases by 23% considering an increase of 10 times the mattress stiffness. At the bottom of the pile, the displacements difference is almost zero.

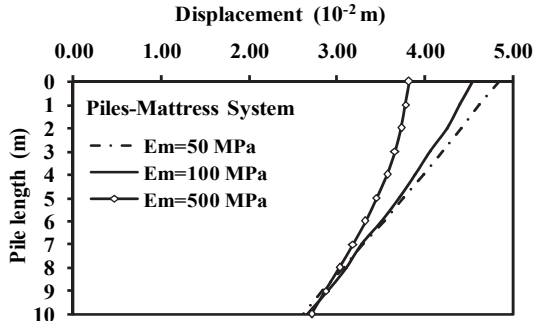

Fig. 11 Influence of the transfer mattress stiffness modulus on the piles-mattress-slab system displacements

The obtained results show that the mattress rigidity affects the internal forces. A slight increase of the bending moments, shear forces and normal forces was observed in Fig. 12. The increase of the internal forces in the piles is proportional to the mattress rigidity increase; this increase was caused by the load transfer to the piles. The wave's propagation velocity inside the mattress becomes higher. The transfer mattress constitutes a energy dissipation zone. When the mattress is rigid, the energy dissipation rate decreases.

4. COMPARISON OF THE ELASTIC AND ELASTO-PLASTIC CALCULATIONS

When entering the field of large deformations, a soil linear behavior is no longer adequate. It is therefore necessary to use non-linear constitutive laws to define the soil behavior surrounding the piles. The introduced constitutive model is the linear elastic perfectly plastic one considering a Mohr-Coulomb failure criterion. The characteristics of this model are presented in Table 1. The last two parameters of the Table 1 are used for the calculations considering an elasto-plastic behavior for the soils.

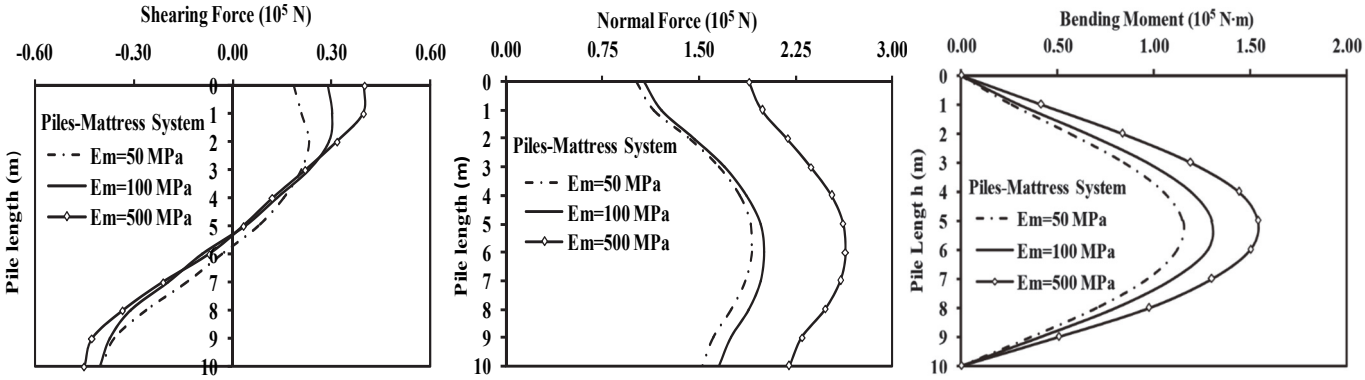

Fig. 12 Influence of the mattress elastic modulus on the internal forces

In this section, only the soil-piles-mattress system is presented. The elasto-plastic calculations were nevertheless done for the two systems. The mattress and soft soil layer were considered as elasto-plastic in the simulations.

A three-dimensional calculation was realized in order to introduce the elasto-plasticity in the analysis of the dynamic behavior of piles-mattress-slab. The calculation was extended to 20 seconds (end of the oscillations). The results of elastic and elasto-plastic calculations are compared for the two system piles-mattress-slab and piles-slab; the piles are rested in the hard soil layer.

Figure 13 shows the internal forces comparison in the elastic and elasto-plastic domains for the piles-mattress and piles-slab systems. Low normal forces are obtained for the elastoplastic models

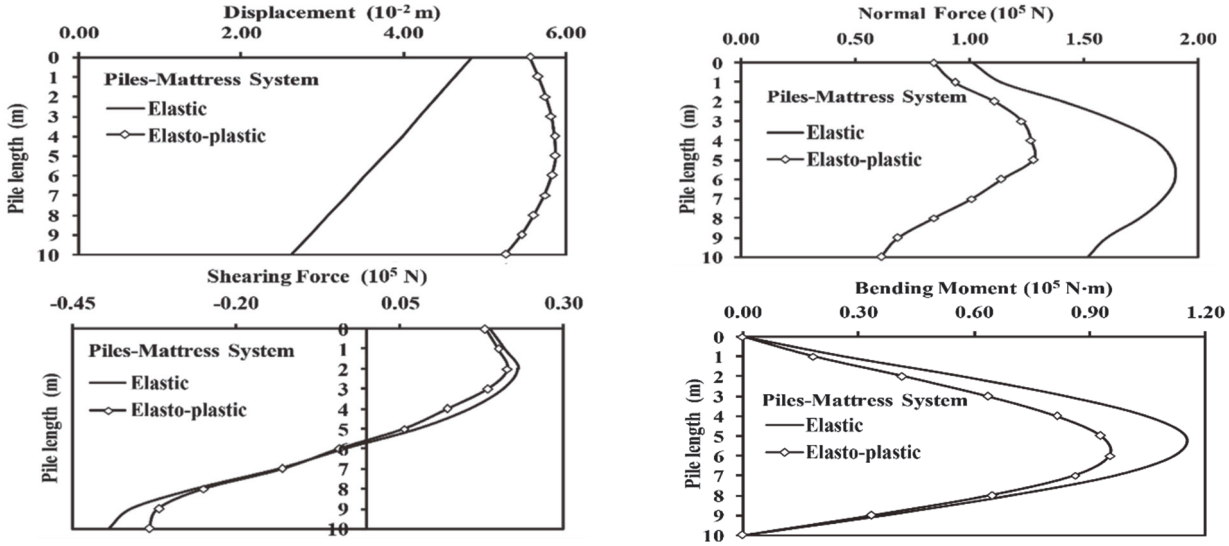

(a) Piles-mattress system

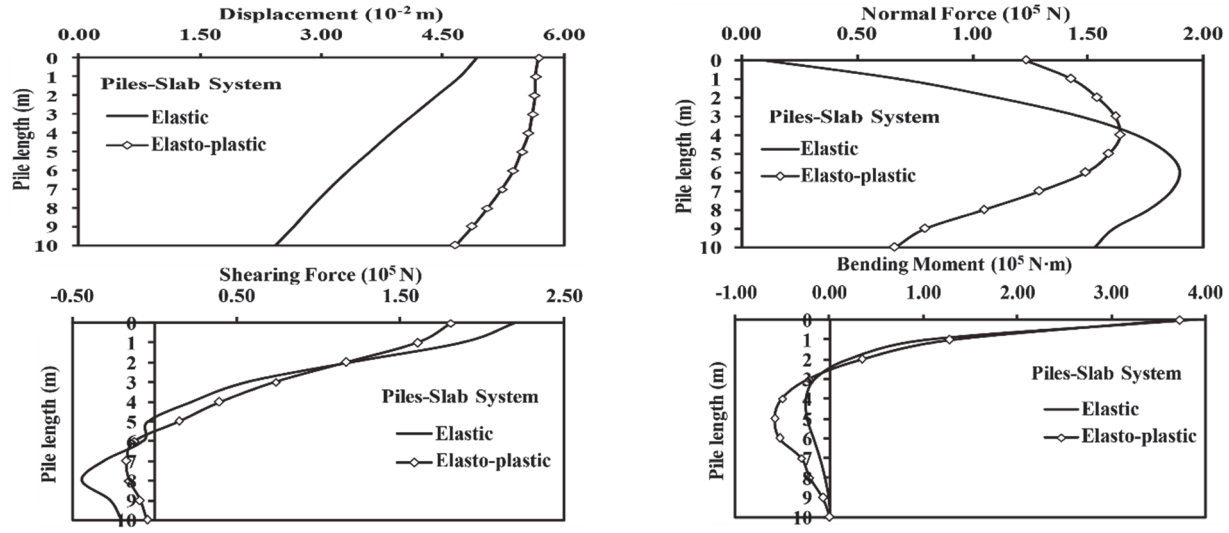

(b) Pile-slab system

Fig. 13 Comparison between the elastic and elasto-plastic results

as the volumic elements surrounding the piles are plastified and do not transmit the compression forces to piles of the reinforcement system. Shear forces and bending moments are greater in the first 6 m of the piles. The displacements and internal forces as a function of A1 pile length for the two soft soil behaviors (elastic and elasto-plastic) are presented in Fig. 13 and Table 5. This figure shows that the displacements in the elastic domain are lower than the elasto-plastic ones. In the elastic domain, the displacement variation is linear but for the elasto-plastic ones it is non-linear; it is due to the soil plastification; in this case the piles are more flexible. The internal forces values (normal force, shearing force and bending moment) in the elastic domain are greater in the elasto-plastic domain. In the elastic domain, the soil behavior is reversible and its resistance is in the opposite direction of the seismic excitation, but in the elasto-plastic field the soft soil can plastify and its resistance is then smaller.

In this analysis, a comparison is made between the internal forces of the soil elastic and elasto-plastic behavior on the row A. The internal forces and displacements are calculated at a depth equal to 5 m of piles for two systems. Figure 14 shows the variation of the internal forces in the direction of the seismic signal.

For studying the piles groups of the piles-mattress and the piles-slab systems, Fig. 14 and Table 6 show an increase of the displacements to the center of the two groups system in the elastic domain. In the elasto-plastic domain, the displacements decrease to the center of the two systems. The behavior in terms of bending moments in the elastic domain is the same as the displacements one. There is an increase of the bending moments to the center of the piles groups. In the elasto-plastic domain, the moments decrease and then increase to the center of the groups system.

The normal force is slightly influenced by the seismic excitation, so this result shows a strong increase of the normal forces on piles-mattress and peripheral piles of the piles-slab. However, the normal force decreases when approaching the center to the groups center for the elastic and elasto-plastic simulations.

For both elastic and elasto-plastic simulations, the shear forces on the axis A are different, one decreases and the other increases for rigid piles. For the piles, there is an increase of the shear forces to the center of the piles groups in the elastic domain. In the elasto-plastic domain, the bending moments once decrease and increase to the center of the groups.

For the same dynamic loading, lower force values are obtained with the elasto-plastic models than with the elastic models. A part of the energy is dissipated in the soil and in contact between the soil and rigid piles.

5. CONCLUSIONS

In this study, a three-dimensional FEM dynamic analysis of the two systems: piles-mattress-slab and piles-slab is presented. The calculations took into account the interaction between the several elements: hard soil, soft soil, piles, slab and mattress. The developed numerical models permitted the calculation of the dynamic internal forces and displacements. This work presents the results of a simulation of soil-rigid piles-mattress-slab and soil-piles-slab systems under seismic loading in terms of displacement and internal stresses (shear force, normal force and bending moment). In addition, a cross analysis was conducted at 5 m piles depth, which allows to make a comparison between piles-mattress and piles-slab systems proposed for the two behaviors (*i.e.* elastic and elasto-plastic).

In the reinforcement system by piles, the more rigid the load transfer mattress is, the more the energy dissipation rate decreases. The shear forces and the moments increase with the increasing of the mattress rigidity. On the other hand, the stresses decrease with the decreasing of the soil stiffness.

Table 5 Comparison between the elastic and elasto-plastic results

			Displacements $\times 10^{-2}$ (m)	Normal forces $\times 10^5$ (N)	Shear forces $\times 10^5$ (N)	Bending moment $\times 10^5$ (N·m)
Piles-slab system	Elastic	0 m	4.92	– 0.0979	2.2000	3.9030
		5 m	3.6	– 1.8506	– 0.0396	– 0.2453
		6 m	3.34	– 1.9045	– 0.0657	– 0.1771
		9 m	2.65	– 1.6117	– 0.2730	– 0.0109
		10 m	2.43	– 1.5326	– 0.2000	0.00034
	Elasto-plastic	0 m	5.68	– 1.2254	1.8126	0.7346
		5 m	5.48	– 1.5927	0.1517	– 0.5880
		6 m	5.37	– 1.4900	– 0.1203	– 0.5339
		9 m	4.86	– 0.7950	– 0.0865	– 0.0719
		10 m	4.65	– 0.6653	– 0.0447	0.0554
Piles-mattress-slab system	Elastic	0 m	4.84	– 1.0105	0.1872	0.00082
		5 m	3.76	– 1.9031	0.0779	1.1500
		6 m	3.53	– 1.9104	– 0.0326	1.1200
		9 m	2.84	– 1.6100	– 0.3593	0.3645
		10 m	2.61	– 1.5311	– 0.3950	0.00076
	Elasto-plastic	0 m	5.56	– 0.8445	0.1816	0.000627
		5 m	5.87	– 1.2457	0.0563	0.9291
		6 m	5.83	– 1.1109	– 0.0420	0.9537
		9 m	5.44	– 0.6882	– 0.3181	0.3365
		10 m	5.26	– 0.6167	– 0.3338	0.000432

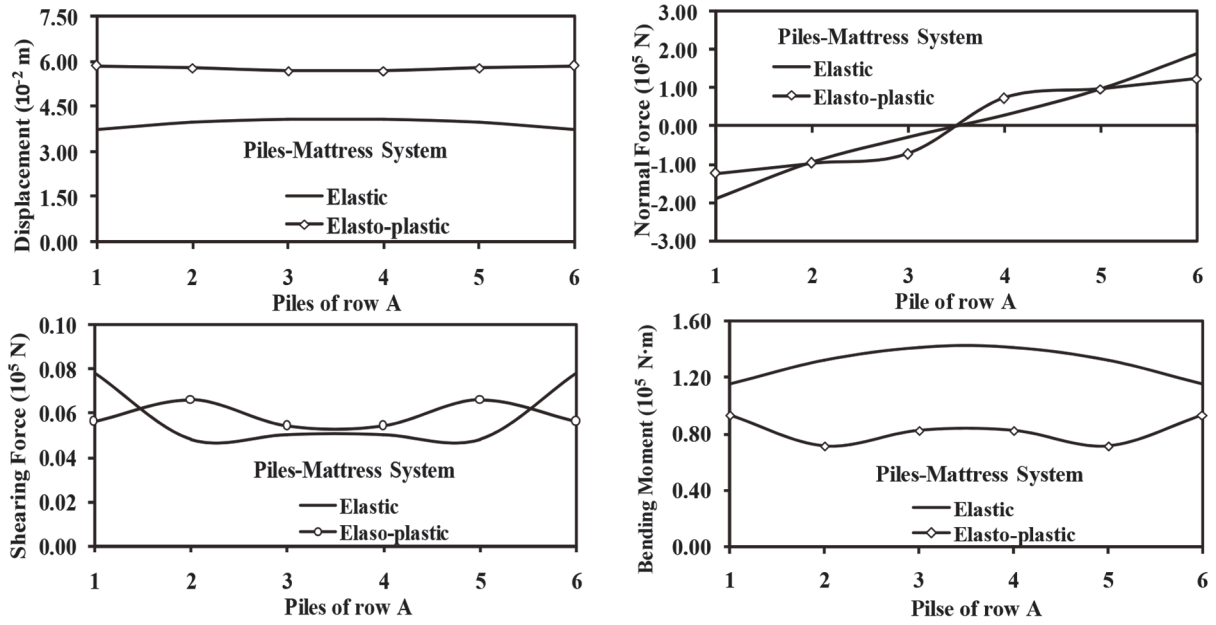

(a) Piles-mattress system

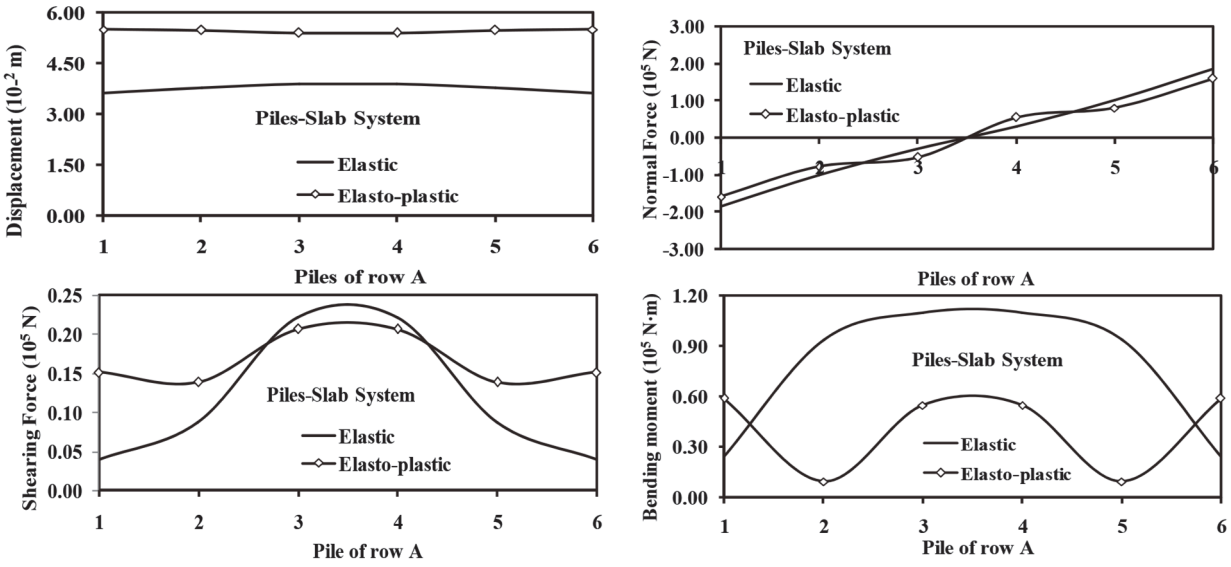

(b) Piles-slab system

Fig. 14 Comparison between the elastic and elasto-plastic results (row A)

Table 6 Elastic and elasto-plastic results (row A)

		Piles	Displacements 10^{-2} (m)	Normal forces $\times 10^5$ (N)	Shear forces $\times 10^5$ (N)	Bending moments $\times 10^5$ (N·m)
Rigid-piles-matress-slab system	Elastic	A1; A6	3.76	– 1.9045	0.0779	1.1500
		A2; A5	3.97	– 0.9590	0.0482	1.3203
		A3; A4	4.08	– 0.2937	0.0504	1.4112
	Elasto-plastic	A1; A6	5.87	– 1.2811	0.0563	0.9291
		A2; A5	5.79	– 0.9720	0.0661	0.7130
		A3; A4	5.70	– 0.7284	0.0543	0.8209
Piles-slab system	Elastic	A1; A6	3.60	– 1.8506	0.0396	0.2453
		A2; A5	3.76	– 1.0100	0.0875	0.940
		A3; A4	3.87	– 0.3128	0.2213	1.100
	Elasto-plastic	A1; A6	5.48	– 1.5927	0.1517	0.5880
		A2; A5	5.45	– 0.7934	0.1381	0.0932
		A3; A4	5.38	– 0.5331	0.2067	0.5475

The displacements and internal stresses of the corner piles of the two systems are compared. The type of connection also influences the internal stresses. The moment at the two ends of the piles of the piles-mattress system and at the bottom of the piles is null due to their articulated connection with the soil. The maximum bending moment value is located at the pile head of the piles-slab system because this node is perfectly connected to the slab.

The stresses in the elastic simulations are greater than in the elasto-plastic ones. In the elastic domain, the soil behavior is reversible and has resistance in the seismic excitation opposite direction. In the elasto-plastic simulations, the soil is deformable and its resistance is smaller.

This study highlights the complex phenomenon of the dynamic response of a reinforced system under seismic loading. This study can be extended to the dynamic response of reinforced system under seismic loading (real earthquake) and under impulsive loading (for road traffics). It will therefore, be necessary to use elasto-plastic models for the soil surrounding the rigid piles.

ACKNOWLEDGMENT

The authors would like to thank the Civil and Environmental Engineering Laboratory, LGCE University of Jijel, Algeria for their technical support. These supports made this study and further research possible.

FUNDING

The authors received no funding for this work.

CONFLICT OF INTEREST STATEMENT

The authors declare that there is no conflict of interest.

DATA AVAILABILITY STATEMENT

The data and/or computer codes used/generated in this study can be downloaded at https://www.code-aster.org/spip.php?rubrique7

REFERENCES

Briançon, L., Dias, D., and Simone, C. (2015). "Monitoring and numerical investigation of a rigid inclusions—reinforced industrial building." *Canadian Geotechnical Journal*, **52**(10), 1592-1604. https://doi.org/10.1139/cgj-2014-0262

Choi, J.S., Yun, C.B., and Kim, J.M. (2001). "Earthquake response analysis of the Hualien soil-structure interaction system based on updated soil properties using forced vibration test data." *Earthquake Engineering and Structural Dynamics*, **30**(1), 1-26. https://doi.org/10.1002/1096-9845(200101)30:1<1::AID-EQE991>3.0.CO;2-Y

Code Aster. http://www.code-aster.org/utilisation/non-french.ph.pNon FrenchCode_AsterResources

Code Aster: définition de Code Aster and synonymes de Code Aster https://dictionnaire.sensagent.leparisien.fr/Code Aster/fr-fr/

Code Aster. *Tool for Interactive Post Processing STANLEY.* https://www.code-aster.org/V2/doc/v13/en/man_u/u4/u4.81.31.pdf

Deb, K., and Mohapatra, S.R. (2013). "Analysis of stone column-supported geosynthetic-reinforced embankments." *Applied Mathematical Modelling*, **37**(5), 2943-2960. https://doi.org/10.1016/j.apm.2012.07.002

Fach, M.A. (2009). *Modélisation tridimensionnelle du Comportement sismique du système sol-pieux-pont: Prise en compte des non-linéarités du sol et du béton*. Thèse de doctorat en Génie civil, universite of Lille 1, https://www.theses.fr/147297028

Gazetas, G. and Dobry, R. (1984). "Horizontal response of piles in layered soils." *Journal of Geotechnical and Geoenvironmental Engineering*, ASCE, **110**(1), 20-40. https://doi.org/10.1061/(ASCE)0733-9410(1984)110:1(20)

Girout, R., Blanc, M., Dias, D., and Thorel, L. (2014). "Numerical analysis of a geosynthetic-reinforced piled load transfer platform—Validation on centrifuge tests." *Geotextiles and Geomembranes*, **42**(5), 525-539. https://doi.org/10.1016/j.geotexmem.2014.07.012

Guéguen, P., Bard, P.Y., and Chavez-Garcia, F.J. (2002). "Site-city seismic interaction in Mexico city like environnement: An analytic study." *Bulletin of the Seismological Society of America*, **92**(2), 794-8011. https://doi.org/10.1785/0120000306

Hassen, G., Dias, D., and De Buhan, P. (2009). "A multiphase constitutive model for the design of piled-embankments: Comparison with three dimensional numerical simulations." *International Journal of Geomechanics*, ASCE, **9**(6), 258-266. https://doi.org/10.1061/(ASCE)1532-3641(2009)9:6(258)

Hatem, A., Shahrour, I., Lambert, S., and Alsaleh, H. (2009). "Analyse du comportement sismique des sols renforces par inclusions rigides et par colonnes a module mixte." *Journées Nationales de Géotechnique et de Géologie de l'Ingénieur JNGG2010- Grenoble.* https://www.cfmr-roches.org/sites/default/files/jngg/JNGG%202010%20pp%20649-656%20Hatem.pdf

Hatem, A. (2009). *Comportement en zone sismique des inclusions rigides. Analyse de l'interaction sol-inclusion-matelas de répartition-structure*. Thèse de doctorat. Université des sciences et de technologies de lille. https://ori-nuxeo.univlille1.fr/nuxeo/site/esupversions/684ac7b4-7

Hung V. Pham. (2018). *3D Modeling of Soft Soil Improvement by Rigid Inclusions-Complex and Cyclic Loading*. Theses, Mechanics of materials [physics.class-ph], Universite Gronoble Alpes.

Hung V. Pham. and Dias, D. (2019). "3D numerical modeling of a piled embankment under cyclic loading." *International Journal of Geomechanics*, ASCE, **19**(4), 04019010. https://doi.org/10.1061/(ASCE)GM.1943-5622.0001354

Jenck, O., Dias, D., and Kastner, R. (2006). "Three-dimensional modelling of an embankment over soft soil improved by rigid piles." *Numerical Methods in Geotechnical Engineering,* Schweiger, H.F., Ed., London: Taylor & Francis, 817-822. https://doi.org/10.1201/9781439833766.CH118

Jenck, O., Dias, D., and Kastner, R. (2007). "Two-dimensional physical and numerical modelling of a pile supported earth platform over soft soil." *Journal of Geotechnical and Geoenvironmental Engineering*, ASCE, **133**(3), 295-305. https://doi.org/10.1061/(ASCE)1090-0241(2007)133:3(295)

Jenck, O., Dias, D., and Kastner, R. (2009a). "Discrete element modelling of a granular platform supported by piles in soft

soil—Validation on a small scale model test and comparison to a numerical analysis in a continuum." *Computers and Geotechnics*, **36**(6), 917-927. https://doi.org/10.1016/j.compgeo.2009.02.001

Jenck, O., Dias, D., and Kastner, R. (2009b). "Three-dimensional numerical modeling of a pile embankment." *International Journal of Geomechanics*, ASCE, **9**(3), 102-112. https://doi.org/10.1061/(ASCE)1532-3641(2009)9:3(102)

Jening, P.C. and Bielak, J. (1973). "Dynamics of building-soil interaction." *Bulletin of Seismological Society of America,* **63**, 9-48. https://doi.org/10.1785/BSSA0630010009

Kagawa, T., Kraft, L.M., Jr. (1980). "Seismic P-Y response of flexibles piles." *Journal of the Geotechnical Engeneering Division*, **106**(8), 899-918. https://doi.org/10.1061/AJGEB6.0001018

Kaynia, A. and Kausel, E. (1982). *Dynamic Stiffness and Seismic Response of Pile Groups*. Research Report R32-03, Massachusetts Inst. of Technologies, Cambridge. https://dspace.mit.edu/bitstream/handle/1721.1/39863/09257395-MIT.pdf?sequence=2

Lysmer, J. and Kuhlemeyer, R.L. (1969). "Finite dynamic model for infinite media." *Journal of the Engineering Mechanics Divisi*on, **95**(4), 859-878. https://doi.org/10.1061/JMCEA3.0001144

Maeso, O., Aznárez, J.J., and García, F. (2005). "Dynamic impedances of piles and groups of piles in saturated soils." *Computers and Structures*, **83**(10-11), 769-782. https://doi.org/10.1016/j.compstruc.2004.10.015

Mayoral, J.M. and Romo, M.P. (2006). "Recent studies on seismic soil-pile-structure-interaction in soft clay." *International Conference on Earthquake Engineering*, Taipei, Taiwan. https://conf.ncree.org.tw/proceedings/i0951012/data/pdf/4ICEE-0034.pdf

Messioud, S., Dias, D., and Sbartai, B. (2019). "Influence of the pile toe condition on the dynamic response of a group of pile foundations." *International Journal of Advanced Structural Engineering*, **11**(1), 55-66. https://doi.org/10.1007/s40091-019-0217-5

Messioud, S., Okyay, U.S., Sbartai, B., and Dias, D. (2016). "Dynamic response of pile reinforced soils and piled foundations." *Geotechnical and Geological Engineering*, **34**(3), 789-805. https://doi.org/10.1007/s10706-016-0003-0

Messioud, S., Okyay, U.S., Sbartai, B., and Dias, D. (2017). "Estimation of dynamic impedance of the soil-pile-slab and soil-pile-mattress-slab systems." *International Journal of Structural Stability and Dynamics*, **17**(6). https://doi.org/10.1142/S0219455417500572

McKay, K. (2009). *Three Applications of the Reciprocal Theorem in Soil-Structure Interaction*. Doctoral Dissertation, University of Southern California. https://www.proquest.com/openview/00986117b0d494c6872b7ec148cbd286/1?pq-origsite=gscholar&cbl=18750

Novak, M. and Aboul-Ella, F. (1978). "Impedance functions of piles in layered media." *Journal of the Engineering Mechanics Division*, **104**(3), 643-661. https://doi.org/10.1061/JMCEA3.0002366

Nunez, M.A., Briançon, L., and Dias, D. (2013). "Analyses of a pile supported embankment over soft clay: Full-scale experiment, analytical and numerical approaches." *Engineering Geology*, **153**, 53-67. https://doi.org/10.1016/j.enggeo.2012.11.006

Okyay, US. (2010). *Etude expérimentale et numérique des transferts de charge dans un massif renforcé par inclusions rigides: Application à des cas de chargements statiques et dynamiques*. Doctoral thesis, Université Lyon 1. https://www.theses.fr/2010ISAL0098

Padrón, L.A., Aznárez, J.J., and Maeso, O. (2007). "BEM-FEM coupling model for the dynamic analysis of piles and pile groups." *Engineering Analysis with Boundary Elements*, **31**(6), 473-484. https://doi.org/10.1016/j.enganabound.2006.11.001

Sen, R., Davis, T.G., and Benrejee, P.K. (1985). "Dynamic analyses of piles and piles groups embedded in homogeneous soil." *Earthquake Engendering and Structural Dynamics*, **13**, 53-65. https://doi.org/10.1002/eqe.4290130107

Stéphane, G. (2008). *Modélisation simplifiée 3D de l'interaction sol-structure: Application en génie parasismique*. Thèse de doctorat. Institut Polytechnique de Grenoble. https://tel.archives-ouvertes.fr/tel-00306842/

Sun, Q., Dias, D., and e Sousa, L.R. (2020). "Soft soil layer-tunnel interaction under seismic loading." *Tunnelling and Underground SpaceTechnology*, **98**, 103329. https://doi.org/10.1016/j.tust.2020.103329

Tajimi, H. (1969). "Dynamic analysis of a structure embedded in an elastic straturn." *Proceedings of the 4th World Conf. on Earth*, EngngIII, 53-69. https://ci.nii.ac.jp/naid/10009397085/

Xilin, Lu., Zhou, Y., and Lu, W. (2003). "Practical model design method of shaking table tests." *Structural Engineers*, **3**, 005. https://doi.org/10.3969/j.issn.1005-0159.2003.03.006

Zhuang, Y. and Wang, K. (2016). "Finite element analysis on the effet of subsoil in reinforced piled embankments and comparison with theoretical method prediction." *International Journal of Geomechanics*, ASCE, **16**(5). https://doi.org/10.1061/(ASCE)GM.1943-5622.0000628

Zhuang, Y. and Wang, K. (2018). "Finite element analysis on the dynamic behavior of soil arching effect in piled embankment." *Transportation Geotechnics*, **14**(27), 8-21. https://doi.org/10.1016/j.trgeo.2017.09.001